Modeling the quasi-optical performance of CMB astronomical interferometers

Gareth S. Curran*[a], Marcin L. Gradziel[b], Créidhe O'Sullivan[b], J. Anthony Murphy [b], Andrei Korotkov [c], Siddharth Malu[d], Peter Timbie[d], Gregory Tucker[c]
[a]Institute of Technology Blanchardstown, Blanchardstown Rd. North, Dublin 15, Ireland;
[b]Experimental Physics Dept., National University of Ireland Maynooth, Co. Kildare, Ireland;
[c]Brown University, Providence, Rhode Island, RI02912;
[d]University of Wisconsin-Madison, Madison, WI53706

ABSTRACT

The Millimeter-Wave Bolometric Interferometer (MBI) is a ground-based instrument designed to measure the polarization anisotropies of the Cosmic Microwave Background (CMB) and contains a number of quasi-optical components, including a complex back-to-back system of corrugated feed-horn antennas. In this paper we use MBI as an example to demonstrate the existing modeling techniques and as a focus to develop extended modeling capabilities. The software we use to model this system targets the millimeter and sub-millimeter region of the electromagnetic spectrum and has been extended to efficiently model the performance of back-to-back corrugated horns embedded in larger optical systems. This allows the calculation of the coupling of radiation from the sky to the detector array through a back-to-back horn feed system.

Keywords: Millimeter-Wave Bolometric Interferometer; CMB; polarization; quasi-optical; coupling; astronomy

1. INTRODUCTION

This paper presents work being done on the optical design and analysis of the beam combiner for the Millimeter-Wave Bolometric Interferometer (MBI), a ground based instrument designed to measure the polarization anisotropies of the Cosmic Microwave Background (CMB) at a central frequency of 90GHz. Interferometry has never before been used to carry out such measurements at this frequency, nor using incoherent bolometers as detectors. MBI will therefore act as a prototype for this type of system and must be modeled in detail to ensure that its operation is fully understood.

The telescope contains a number of quasi-optical components, including a complex back-to-back system of corrugated feed horn antennas. Knowledge of the optical performance and beam patterns of such a system is critical for understanding systematic effects in the reliable extraction of feasible polarization signals.

To model the system accurately we have employed a variety of both commercial and in-house software packages. MODAL [1], an optical design and analysis package developed at NUI Maynooth and targeting the millimeter and sub-millimeter region of the electromagnetic spectrum was used most widely. This not only allows the initial design and preliminary analysis of the multi-element optical system to be carried out in a computationally efficient manner using quasi-optical techniques but also enables a complete electromagnetic characterization using Physical Optics. We describe the techniques used, their predictions and the performance of the telescope as calculated to-date.

2. POLARIZATION AND THE COSMIC MICROWAVE BACKGROUND

The Cosmic Microwave Background is the relic radiation from the Big Bang and exhibits very faint temperature anisotropies indicative of the primordial density fluctuations of the early universe. The temperature power spectrum has been well characterized over a broad range of angular scales, however it is now realized that temperature measurements

*gareth.curran@itb.ie; phone 00353 1 8851097

Millimeter and Submillimeter Detectors and Instrumentation for Astronomy IV
edited by William D. Duncan, Wayne S. Holland, Stafford Withington, Jonas Zmuidzinas
Proc. of SPIE Vol. 7020, 70202O, (2008) · 0277-786X/08/$18 · doi: 10.1117/12.790500

alone are not sufficient to uniquely constrain the cosmological constants required for detailed modeling.

A more comprehensive analysis shows that there are anisotropies in the linear polarization of the CMB which are introduced by Thompson scattering of photons at re-ionization. This was first detected by the Degree Angular Scale Interferometer (DASI) experiment [2] in 2002. Accurate measurements of this polarization are expected to lead to tighter constraints on cosmological parameters describing the density, composition and expansion rate of the universe and the latest generation of experiments, such as QUaD [3], PLANK [4] and MBI [5], are only now approaching the sensitivity needed to carry out these measurements. CMB polarization is generally decomposed into two coordinate-independent components, called E- and B-modes. Physically, this decomposition is useful because scalar perturbations (fluctuations in the gravitational potential) produce only E-modes whereas tensor perturbations (distortions in the metric) produce both E- and B-modes. Although polarized power has been detected in the CMB, no high-signal-to-noise maps have been made and no B-modes have been detected.

3. THE MILLIMETRE-WAVE BOLOMETRIC INTERFEROMETER

3.1 Background

The Millimeter-Wave Bolometric Interferometer is a Fizeau interferometer that uses cooled spider web bolometers for detectors, combining the advantages of interferometry for control of systematic effects with the high sensitivity and frequency coverage possessed by bolometers [6]. It is the first bolometric interferometer of its kind which results in a novel instrument with capabilities that would be difficult to achieve using more traditional techniques and will allow MBI and instruments based on its technology to explore a wide range of angular scales and wavelengths. Unlike a single-dish imaging telescope, an interferometer instantaneously performs a differential measurement with the effective beam pattern of each individual baseline being a set of fringes that sample the sky with positive and negative weights. This differencing removes the need for mechanical chopping or rapid scanning.

The prototype MBI instrument has four interferometer apertures and uses nineteen bolometers. This prototype is called MBI-4 and operates at a central frequency of 90 GHz. The configuration used in this system may be expanded to an N=8 instrument with eight apertures and it is proposed to ultimately design and build a 64-element interferometer or N=64 configuration (MBI-64). MBI-64 will operate as either eight N=8 interferometers in parallel or as one N=64 system. As a prelude to MBI-4, both a room temperature and a cryogenic interferometer called the MBI Test Bed (MTB) were demonstrated and successfully produced interference fringes as desired. MBI-4 has also undergone demonstration and test observations at Pine Bluff Observatory, Cross Plains, Wisconsin before it is to be used for full scale scientific observations and measurements.

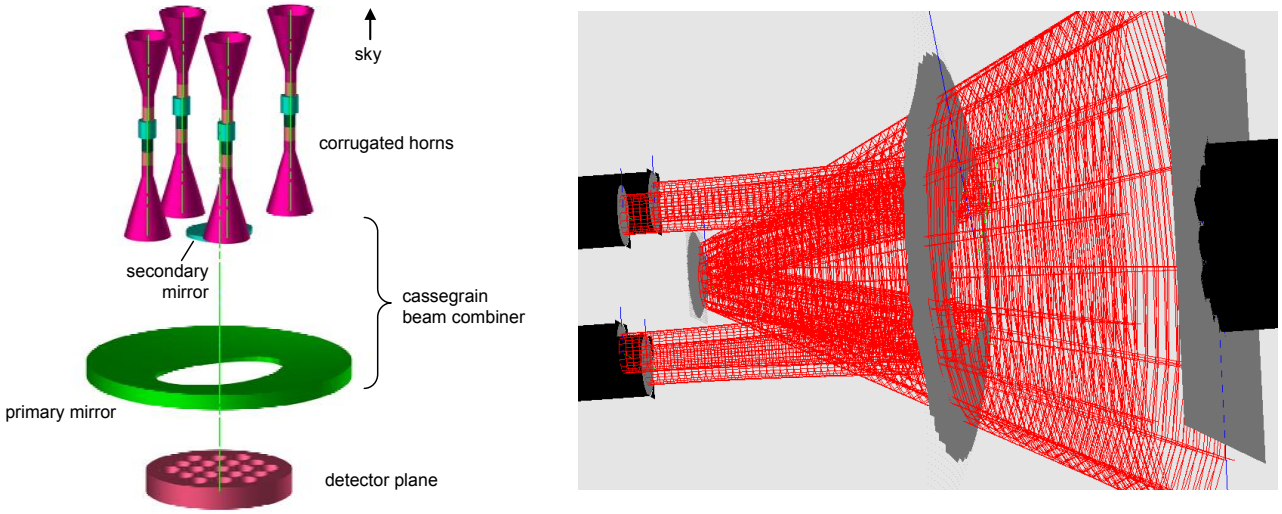

Fig. 1. An artists impression of the Millimeter-Wave Bolometric Interferometer (left) and the telescope as modeled in MODAL (right). The back-to-back feed system that illuminates the primary mirror can be clearly seen, as can the detector plane consisting of 19 spider-web bolometers. Because of the positioning of the of the horn antennas the aperture in the primary can be seen to be elliptical, however truncation at the primary still occurs.

3.2 The Telescope

MBI-4, the first generation of the instrument, is an adding interferometer that views the CMB through 4 corrugated conical horn antennas. At present, for test measurements, this system has been simplified to 4 corrugated conical horns fed by fundamental-mode circular waveguides. Each antenna selects a single linear polarization and the signals are correlated using a cryogenic beam-combining telescope (Fizeau combiner) consisting of a parabolic primary mirror (300mm diameter) and a hyperbolic secondary mirror (64mm diameter). Due to the constraints on the optical design and the overall size of the primary mirror, the aperture in this mirror is elliptical in shape in an effort to strike a balance between preventing truncation of the beams from the illuminating feed horns and allowing the best possible transmission of the beam after reflection at the secondary mirror. The signals from each baseline form an interference fringe pattern in the focal plane on an array of 19 spider-web bolometers which are fed by conical horns. Phase-modulation of the signal from each antenna modulates the fringes in the focal plane and allows lock-in detection of the visibilities [7].

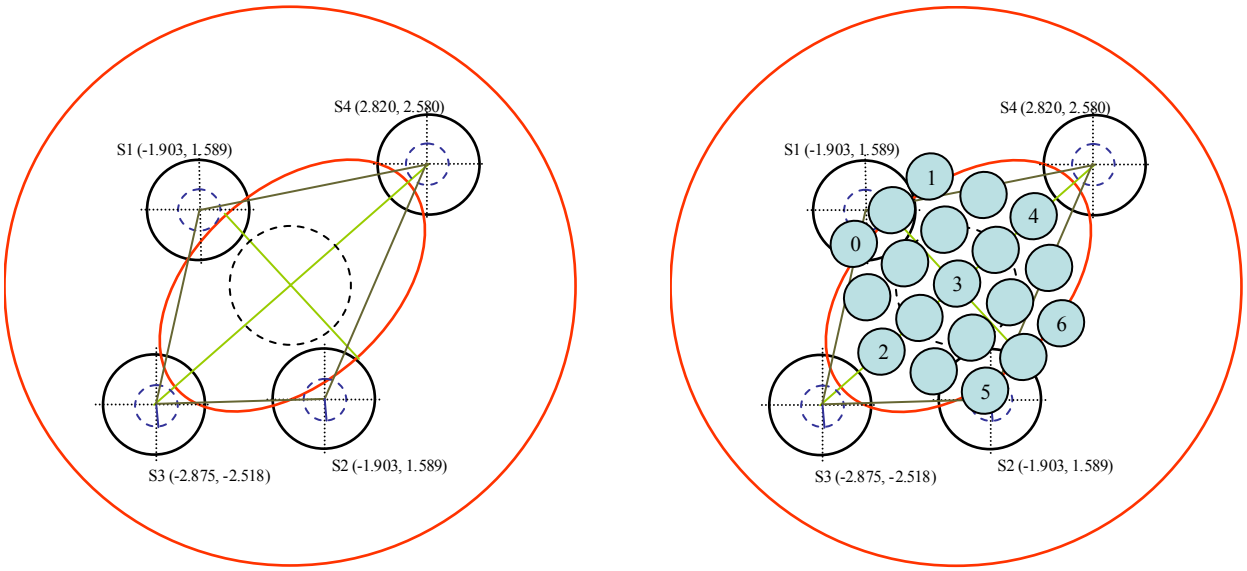

Fig. 2. Schematic diagram showing the optical layout of the MBI beam combining telescope. The left image shows the position of the 4 illuminating corrugated horn antennas with respect to the primary and secondary mirrors. The right image indicates the position of the detector array of 19 spider-web bolometers (the numbers are referred to later).

4. ANALYSIS TECHNIQUES

4.1 Ray Tracing and the Initial Optical Design

The design of the beam combining telescope was carried out by NUI Maynooth, however the positions of the illuminating feed horn antennas and the detector plane were already fixed and therefore there were significant constraints on the layout of the optical system. Also, it was essential that the correct number of interference fringes were created on the detector array to ensure that the signal was properly sampled by this array (i.e. at least two samples per fringe). A ray tracing analysis was used as a first approximation to verify the design and to ensure that the centre of the beams struck the mirrors and converged in the appropriate areas, such as at the secondary mirror and on the array of detectors at the image plane. This analysis was carried out using ZEMAX®, a commercially available program specifically designed for ray tracing.

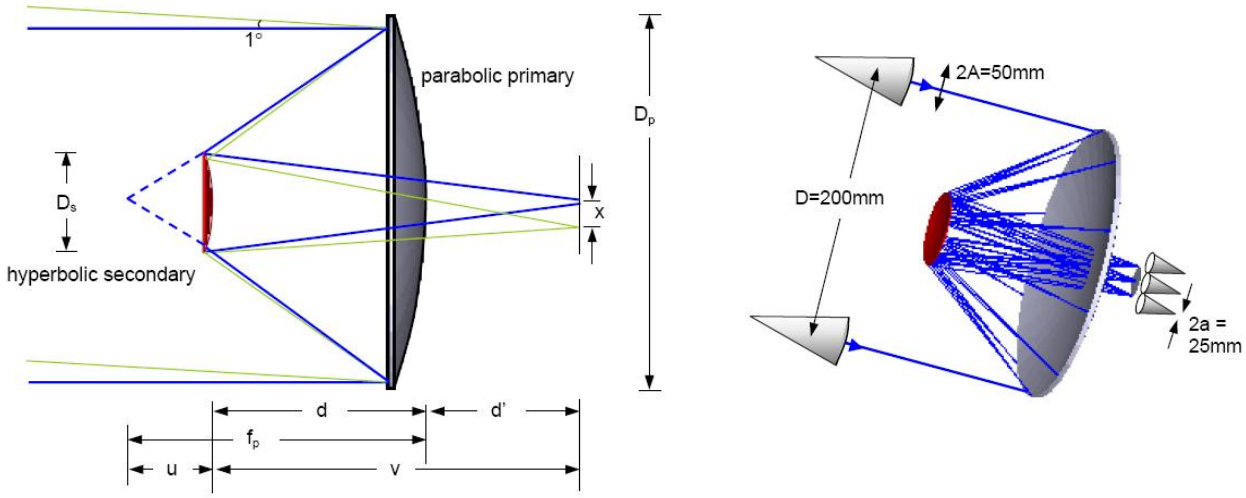

Fig. 3. Schematic diagram of the MBI optical system where D_P is the diameter of the primary mirror, D_S is the diameter of the secondary mirror, d is the distance between the mirrors, d' is the distance from the primary to the image plane, f_P is the primary focal length, f_S is the secondary focal length, x is the fringe separation, D is the baseline, A is the radius of the feed horn and a is the radius of the detector horn [8].

If we consider the system shown in Figure 2 with an operating frequency of 90GHz (λ=3.3mm) and a baseline of 200mm, then the resolution achieved is approximately 1° (λ/D). Since the MBI detector horns are approximately 25mm in diameter and we want two samples per fringe, then the fringe width must equal 50mm. To calculate the equivalent focal length for the system we use the fact that,

$$\frac{x}{f} = \tan\left(\frac{\lambda}{D}\right) \approx \left(\frac{\lambda}{D}\right) \tag{1}$$

giving a focal length of 3000mm and an F/15 (f/D) beam at the output plane. Once the required focal length of the system was known, the values for the primary and secondary focal lengths and the distance between the primary and secondary mirrors could be chosen. However, it was essential that they satisfied the equation

$$\frac{1}{f} = \frac{1}{f_P} + \frac{1}{f_S} - \frac{d}{f_P f_S} \tag{2}$$

Having taken into account the constraints on the optical system with regards to both physical space and the parameters outlined above, the values shown in Table 1 below were chosen. If these are substituted into Equation 2 above, the equivalent focal length obtained is 3000mm, as required to achieve the correct resolution for the given baseline.

Table 1. Properties of the MBI beam combining telescope optical components.

Optical Properties of the MBI Telescope	
Resolution	1° (50mm)
Primary focal length	228.57mm
Secondary focal length	-30.93mm
Distance from primary to secondary	200mm

To test this design further a more rigorous analysis was required. This was carried out using a range of methods such as Gaussian Beam Mode analysis and Physical Optics. The field generated by the feed horn antennas was calculated using a mode-matching technique. Progress was also made on the road to comprehensive modeling of the back-to-back horn structure, with the goal of full sky-to-detector modeling of MBI in NUI Maynooth's software – MODAL.

4.2 Modal Analysis and Singular Value Decomposition

Modal analysis techniques are often an efficient alternative to methods such as Physical Optics or Finite Element Analysis, depending on the type of system considered. The radiation propagating through a uniform section of the system is represented as a linear combination of appropriate modes Ψ_i (for example waveguide modes in a waveguide section or Gaussian Beam Modes in free space), with known propagation characteristics:

$$\Psi = \sum_i A_i \Psi_i \tag{3}$$

The mode amplitudes Ai can be determined by calculating the overlap integrals between the initial field and the individual modes.

The effect of discontinuities in the system (for example a change in the radius of the waveguide, or a quasi-optical element) on the mode amplitudes is given in terms of their scattering matrix S:

$$[B] = [S][A] \tag{4}$$

where *B*i are the new mode amplitudes, typically corresponding to a new outgoing set of modes. The scattering matrix represents the coupling between the incident and outgoing modes and scattering matrices for consecutive elements are cascaded to determine the overall scattering matrix for the system.

The main difficulties in modal analysis are: selection of the most appropriate set of modes, calculation of scattering matrices, and the initial mode coefficients.

4.3 Gaussian Beam Mode Analysis

Gaussian Beam Mode analysis is an example of a modal method, particularly suited for modeling propagation in free space. It was originally developed for use with lasers but was found to be both conceptually and computationally superior to diffraction integral techniques in the analysis of millimeter/submillimetre-wave quasi-optical systems [9]. In this method the radiation is treated as a monochromatic spatially coherent beam represented by the complex scalar field $E(x,y,z)$. This beam can be considered to be composed of a linear combination of independently propagating self-diffracting complex modes with transverse amplitude distribution whose envelope is a Gaussian function [10]. These modes are solutions to the wave equation appropriate to quasi-optical propagation and can be propagated independently through the system before being recombined at a particular plane, such as the image plane.

In the case of the Gaussian Beam Mode analysis of quasi-optical systems it is possible to select a finite set of modes that are a nearly complete basis of the propagating beam. This allows the calculation of the mode coefficients through the overlap integrals to be replaced by least squares fitting of a linear combination of modes to the known field on a relatively small number of sample points, which can be significantly more efficient. To improve the robustness of this approach the best fit coefficients are calculated using truncated SVD decomposition of the matrix representing the sampled modes. This helps to minimize problems caused by non-orthogonality of the sampled representations of the modes, which can be caused by actual non-orthogonality of the modes on curved surfaces, or by inadequate sampling. SVD analysis allows the effective rank of the mode matrix to be discovered and remove the problematic modes from the decomposition [11].

4.4 Waveguide Structures

One of the aims of this work was to develop efficient modeling capability for waveguide components embedded in a bigger optical system. This is an extension of NUI Maynooth's mode matching software, SCATTER [12]. The software models a waveguide structure as a series of cylindrical waveguide sections and uses an electromagnetic mode-matching technique to analyze scattering between propagating and evanescent waveguide modes at each waveguide junction. The scattering matrices representing the junctions and the straight sections are then cascaded to produce the scattering matrices for the structure. Four matrices are needed to fully characterize a structure with 2 ports (S_{11}, S_{21}, S_{12}, S_{22}; first index is the output port, second is the input port, for example S_{21} represents forward propagation from port 1 to port 2).

In the analyses of MBI, SCATTER was initially only used to calculate the field at the aperture of the feed horns, which was then propagated and coupled to the detector horns. In this case the throat of the horn acts as a filter and only a small number of input modes (1 for a single-moded horn) needed to be considered. The column(s) of S_{21} gives the corresponding combinations of the output waveguide modes at the mouth of the horn, and therefore the beam pattern.

In a waveguide structure embedded in a free space quasi-optical system, a back-to-back system, the section that acts as a filter is in the centre and therefore the number of independent modes that can propagate through the system is much smaller than the number of modes that need to be considered at the input. Therefore, the most efficient way of modeling the coupling and propagation through the structure of the radiation incident on the input port is to determine the combinations of input modes that give rise to non-zero output mode combinations. Only those few combinations then need to be coupled with the incident field. Singular Value Decomposition of the scattering matrix can be used to find those effective modes at both ports, as well as their attenuation as they propagate through the structure.

SVD decomposes an $m \times n$ matrix **S** into the following product [13],

$$[S] = [U][W][V]^T \tag{5}$$

where **U** is an $m \times m$ orthogonal matrix, **V** is an $n \times n$ orthogonal matrix and **W** is an $m \times n$ rectangular matrix with real, nonnegative diagonal elements, σ_i. By convention, the diagonal elements of **W**, which are referred to as the singular values of **S**, are non-negative and arranged in decreasing order [14].

The columns of **U** corresponding to non-zero singular values are an orthonormal set of basis vectors that span the range of output modes, while the same columns of **V** are an orthonormal set of basis vectors that span the range of input modes [15]. This means that

$$[S][v_i] = \sigma_i [u_i] \tag{6}$$

In the analysis of a back-to-back waveguide structure only a small number of singular values are effectively non-zero and their corresponding columns of the **V** matrix give us the only independent combinations of the input waveguide modes that need to be considered. Figure 4 shows an example result for a simplified back-to-back system using MBI horns. If the coupling coefficient between the incident field and the effective mode given by $\mathbf{V_i}$ is α_i, the resulting combination of waveguide modes at the output port is given by $\alpha_i \sigma_i [u_i]$. At this point the corresponding aperture field can be calculated and propagated back out into free space.

The gain in efficiency from using the singular vectors is greatest when the same scattering matrix can be used with a number of input fields, say corresponding to different angles on the sky. However, if the input field remains constant, and the scattering matrix changes between simulations, for example because of the scan of the phase shift in the channel, it will generally be more efficient to couple the incident field to individual waveguide modes and use the full scattering matrix.

Work is currently ongoing on extending the core SCATTER code to allow calculation of scattering matrices for more complex structures, consisting of a combination of various cylindrical and rectangular waveguide components, with the appropriate transitions. This will allow a full simulation of the MBI optics to be performed within MODAL.

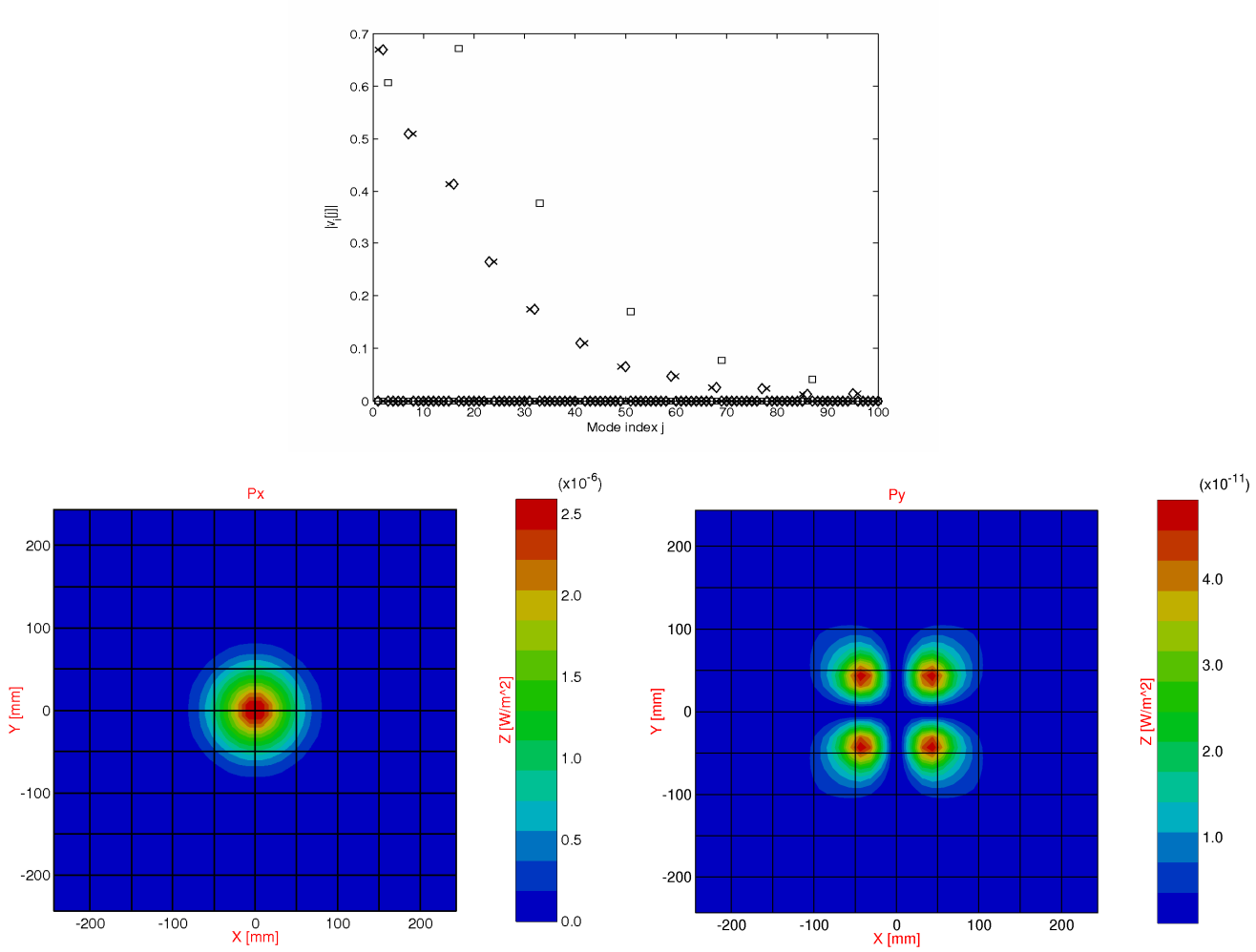

Fig. 4. Example of SVD reduction of the scattering matrix of a waveguide structure. Two MBI horns were modeled back to back with an extra 18 mm straight circular waveguide section between them. At 90 GHz three modes can propagate through this system: two corresponding to the two orthogonal polarizations of the fundamental hybrid mode (crosses and diamonds; singular value 0.9996), and the third to an effective mode consistent with TM_{01} mode in the straight section (squares; singular value 0.4229). This third mode does not couple to the incident radiation, and the outgoing beam pattern is given by the fundamental hybrid mode. The beam pattern shown here (co-polar left and cross-polar right) correspond to the output plane 0.8 m behind the input aperture of the back-to-back system, illuminated by a plane wave with E amplitude 1 V/m incident at 10°. A total of 709 modes, propagating and evanescent modes (not all shown) with azimuthal orders from 0 to 4, ordered according to their cutoff frequencies were included in the scattering matrix.

5. RESULTS

A number of calculations were carried out on the MBI optical system. Firstly, the power coupled to the detectors from each of the source horn antennas was calculated and this value was quite low compared to the power injected into the system. It was therefore essential to find where the power was being truncated by monitoring the transmitted power at different planes in the system. Table 2 contains the results of this analysis, showing the fraction of the source power at each plane.

Table 2: The transmitted power at different planes in the MBI optical system.

The Power Transmitted at Different Planes in the MBI Optical System				
Point in System	Power (W)			
	Source 1	Source 2	Source 3	Source 4
Source	1	1	1	1
Secondary Transmission	0.999542	0.999551	0.999624	0.999624
Primary Reflection	0.894243	0.835838	0.920831	0.921858
Secondary Reflection	0.86939	0.804995	0.889668	0.890841
Primary Transmission	0.273388	0.233216	0.29192	0.292775
Image	0.269604	0.229971	0.28785	0.2887

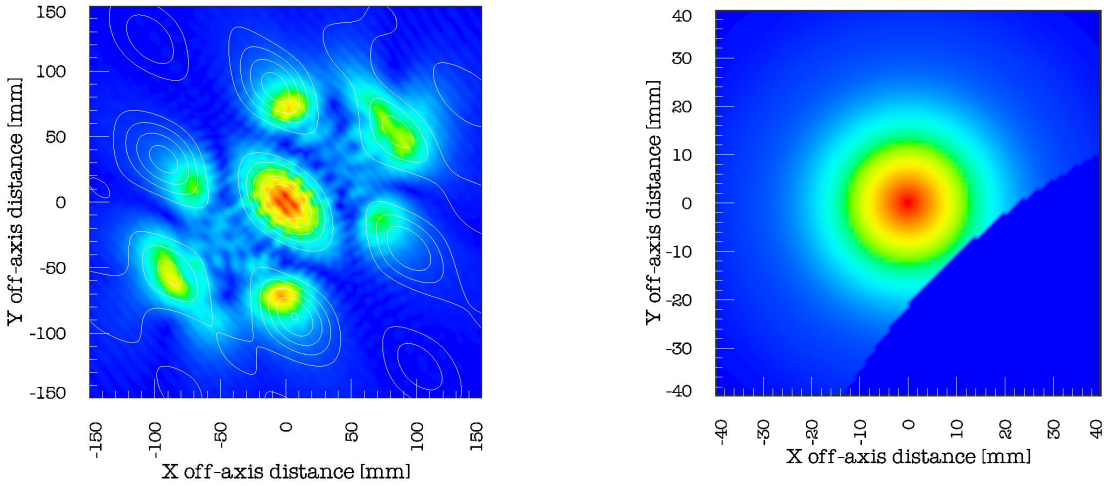

Fig. 5. The field at the image plane of the telescope (left) where the contours show the intensity with no truncation at the primary aperture and the color map takes into account this truncation. The truncated beam from a single source on reflection at the primary mirror (right).

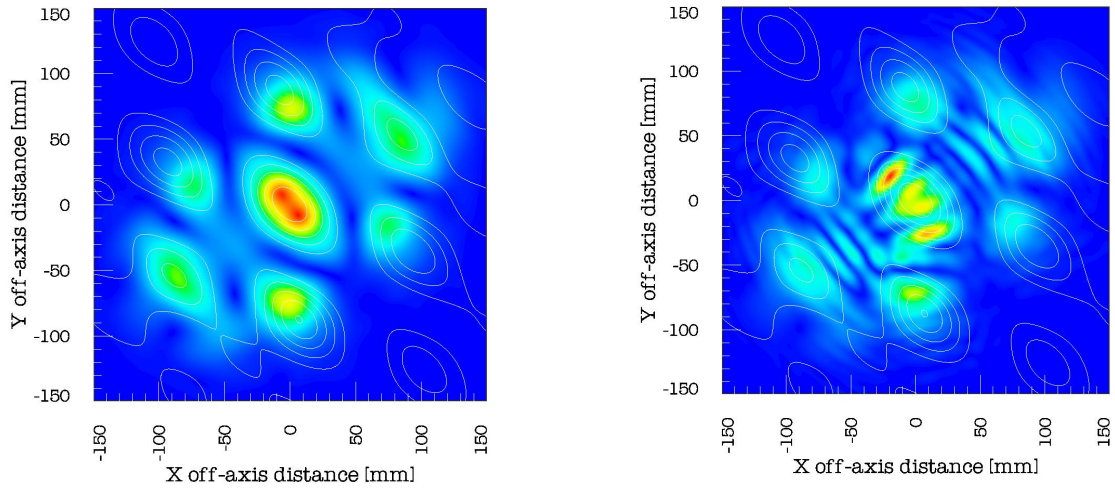

Fig. 6. The field at the image plane with the color map representing a Gaussian beam mode analysis and the contours a physical optics analysis (left). A Gaussian beam mode analysis with the field that passes through the aperture on reflection at the primary taken into account (right).

It can be clearly seen that most of the power is being lost at transmission through the elliptical aperture of the primary mirror after reflection from the secondary. This was further demonstrated by plotting the electric field at the image plane both with and without truncation by the primary aperture as shown in Figure 5. Also, Table 2 shows that approximately 10% of the power from each source is truncated at reflection from the primary mirror due to a fraction of the beam passing straight through the aperture which therefore does not get reflected, as shown above (Figure 5). The effect of this section of the beam passing straight through the primary aperture on the first pass is substantial as shown in Figure 6. It was also shown that for computational efficiency a Gaussian beam mode analysis could be used to predict the beam patterns at the detector plane with a high degree of accuracy.

As well as truncation, the effects of mechanical tolerances in the form of misalignment were also investigated. Figure 7 shows the amplitude and phase of the coupled field between the four source horn antennas and the numbered horn antennas in Figure 2 above, with the analysis being carried out for both a lateral and longitudinal displacement of 1mm (towards the optical system for longitudinal), which by corrected by subtracting the phase shift corresponding to the change in propagation distance. The effect of this misalignment is more significant for the phase than for the amplitude and is also more pronounced in the case of lateral movement.

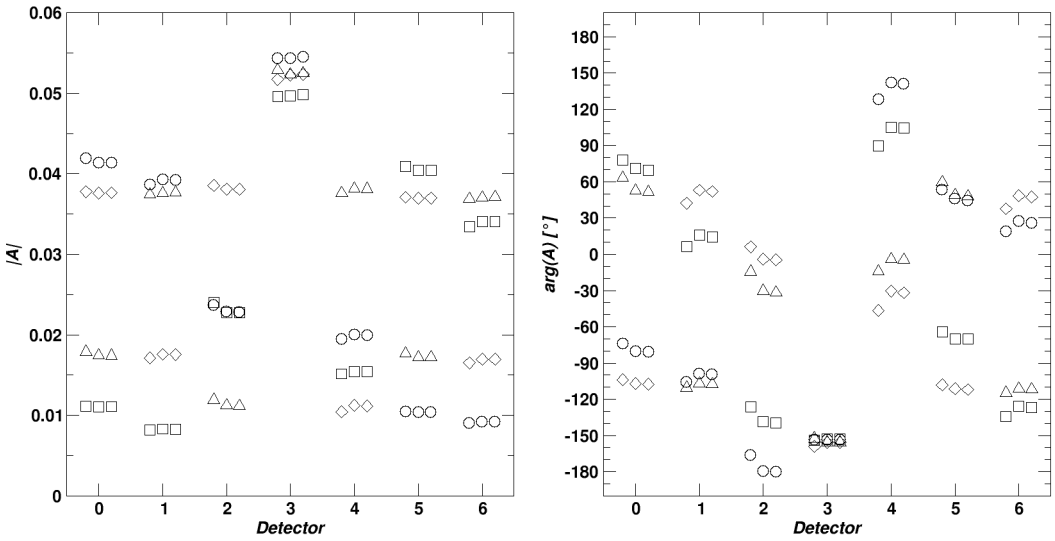

Fig.7. The amplitude (left) and phase (right) of the coupled field between each of the four source horn antennas and a selection of detectors in the detector array (see Figure 2) taking into account mechanical tolerances with regards to positioning. The left-most symbol for each point represents lateral displacement by 1mm while the right-most symbol represents longitudinal displacement by 1mm (towards the optical system) of the detector array, correct by subtracting the phase shift corresponding to the changed propagation distance. Also, within each graph, source 1 is indicated by a circle, source 2 by a square, source 3 by a diamond and source 4 by a triangle.

ACKNOWLEDGEMENTS

This work was supported in part by Science Foundation Ireland (SFI) under its Research Frontiers Program. The development of MODAL was also supported by SFI.

REFERENCES

[1] Gradziel, M. L., O'Sullivan, C., Murphy, J. A., Cahill, G., Curran, G. S., Pryke, C., Gear, W., Church, S., "Modeling of the optical performance of millimeter-wave instruments using MODAL", Proc. SPIE Vol.6472, 64720D.

[2] Kovac, J., Leitch, E. M., Pryke, C., Carlstrom, J. E., Halverson, N. W., Holzapfel, W. L., "Detection of polarization in the cosmic microwave background using DASI", Nature, 420, 772, (2002).

[3] Church, S. et al., "QUEST on DASI: a South-Pole CMB polarization experiment", New Astron. Rev., 47, 1083-1089, (2003).

[4] Lamarre, J. M., et al., "The Planck High-Frequency Instrument, a Third generation CMB Experiment, and a Full-Sky Submillimeter Survey", New Astron. Rev., 47, 1017-1024, (2003).

[5] Timbie, P. T., Tucker, G. S., Ade, P. A. R., Ali, S., Bierman, E., Bunn, E. F., Calderon, C., Gault, A. C., Hyland, P. O., Keating, B. G., Kim, J., Korotkov, A., Malu, S. S., Mauskopf, P., Murphy, J. A., O'Sullivan, S., Piccirillo, L., Wandelt, B. D., "The Einstein polarization interferometer for cosmology (EPIC) and the millimeter-wave bolometric interferometer (MBI)", New Astron. Rev., 50, 999-1008, (2006).

[6] Korotkov, A., Kim, J., Tucker, G. S., Gault, A. C., Hyland, P. O., Malu, S. S., Timbie, P. T., Bunn, E., Bierman, E., Keating, B., Murphy, J. A., O'Sullivan, C., Ade, P. A. R., Calderon, C., Piccirillo, L., "The Millimeter-Wave Bolometric Interferometer", Proc. SPIE Vol.6273.

[7] O'Sullivan, C., Murphy, J. A., Yurchenko, V., Cahill, G., Curran, G. S., Gradziel, M. L., Lavelle, J., Noviello, F., "The Quasi-Optical Performance of CMB Astronomical Telescopes" Proc. SPIE Vol.6472, 647202.

[8] O'Sullivan, C., "Report on the design of MBI", MBI Internal Report No.1, (2005).

[9] Siegman, A.E., "Lasers" University Science Books, California, (1986).

[10] Lesurf, J. C. G., "Millimetre-Wave Optics, Devices and Systems", Institute of Physics Press, (1993).

[11] Gradziel, M. L., White, D., Withington, S., Murphy, J. A., "Fast CAD Software for the Optical Design of Long Wavelength Systems", IRMMW-THZ, Williamsburg, Virginia, USA, pp. 237-8, (2005).

[12] Murphy, J. A., Colgan, R., O'Sullivan, C., Maffei, B., Ade, P. A. R., "Radiation patterns of multi-moded corrugated horns for far-IR space applications", Infrared Physics and Technology, 42, pp 515-528, (2001).

[13] Withington, S., Hobson, M. P., Berry, R. H., "Representing the behavior of partially coherent optical systems by using overcomplete basis sets", J. Opt. Soc. Am. A, Vol. 21, No. 2, February, (2004).

[14] White, D., "The Development of Efficient CAD Software for Terahertz Optical Design and Analysis", Ph.D. Thesis, National University of Ireland, Maynooth, Ireland, (2006).

[15] Press, W. H., Flannery, B. P., Teukolsky, S. A., Vetterling, W. T., "Numerical Recipes – The Art of Scientific Computing", Cambridge University Press, (1986).